

Supporting Information

Cooperativity and ion pairing in magnesium sulfate aqueous solutions from the dilute regime to the solubility limit

Federico Sebastiani^{1,+}, Ana Vila Verde², Matthias Heyden^{3,*},
Gerhard Schwaab^{1,*}, and Martina Havenith^{1,*}

¹Department of Physical Chemistry II, Ruhr-University Bochum,
Bochum, Germany

²Department of Theory & Bio-systems, Max Planck Institute for
Colloids and Interfaces, Potsdam, Germany.

³School of Molecular Sciences, Arizona State University, Tempe,
AZ, USA

⁺Present Address: Department of Chemistry "U. Schiff",
University of Florence, Sesto Fiorentino, Italy

^{*}Corresponding authors; E-mail: mheyden1@asu.edu;
gerhard.schwaab@rub.de; martina.havenith@rub.de

May 8, 2020

Calculated absorption spectra of bulk water and MgSO₄ solutions

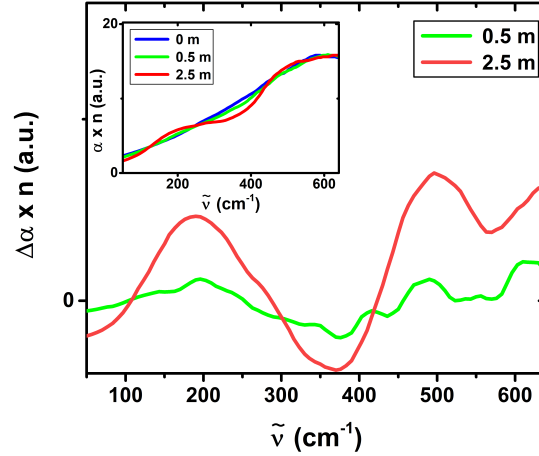


Figure S1: Differential absorption spectra between MgSO₄ solutions and pure water, as obtained from the simulations, corrected for the effective volume of water in the solution. The inset shows the theoretical total absorption spectra of bulk water and MgSO₄ solutions at $m = 0.5 \text{ mol}\cdot\text{kg}^{-1}$ and $m = 2.5 \text{ mol}\cdot\text{kg}^{-1}$ (also shown in Figure 1(B) of the main text and reproduced here for the convenience of the reader).

The quantity calculated in the simulations is $\alpha(\tilde{\nu}) \times n(\tilde{\nu})$, as shown in the inset of Figure S1. The differential absorption spectra between MgSO₄ solutions and pure water ($\Delta\alpha \times n = \alpha_{sol} \times n_{sol} - \frac{c_w}{c_0} \cdot \alpha_{bulk} \times n_{bulk}$) shown in the same figure are corrected for the different water concentration in the solution relative to the bulk, according to Eqs. 2 in the main text and Ref.¹. To enable a direct comparison with experiment, the differential absorption spectra shown in Figure 1 in the Main Text was further corrected for the refractive index change between water and salt solutions, as described below.

The estimation of the refractive index at 90 GHz was carried out from the data in Ref. Mamatkulov *et al.*² as:

$$\begin{aligned} \epsilon(\tilde{\nu}) &= \epsilon'(\tilde{\nu}) + i\epsilon''(\tilde{\nu}) = (n + ik)^2 \\ n^2(\tilde{\nu}) &= \frac{1}{2}(\epsilon'^2(\tilde{\nu}) + \epsilon''^2(\tilde{\nu}))^{\frac{1}{2}} + \epsilon'(\tilde{\nu}) \\ k^2(\tilde{\nu}) &= \frac{1}{2}(\epsilon'^2(\tilde{\nu}) + \epsilon''^2(\tilde{\nu}))^{\frac{1}{2}} - \epsilon'(\tilde{\nu}) \end{aligned} \tag{S.1}$$

where $\epsilon(\tilde{\nu})$ is the complex dielectric constant, while ϵ' and ϵ'' , $n(\tilde{\nu})$ and $k(\tilde{\nu})$ are the real and imaginary parts of the dielectric constant and of the refractive index, respectively.³

The refractive index of MgSO_4 solutions at $0.8 \text{ mol}\cdot\text{dm}^{-3}$ and $2.2 \text{ mol}\cdot\text{dm}^{-3}$ have been calculated to be 3.7 % and 9 % lower than that of water, respectively. We extrapolated those values of the refractive index to the concentrations considered here, obtaining a difference with respect to bulk water of 2 % for $0.5 \text{ mol}\cdot\text{dm}^{-3}$ and of 10 % for $2.4 \text{ mol}\cdot\text{dm}^{-3}$ solutions, respectively. These quantities were assumed to be frequency-independent, as the refractive index is not expected to vary significantly in this frequency range⁴.

Thus, the effective differential absorption spectra in Figure 1(B) of the main text were calculated as:

$$\Delta\alpha_{eff}(\omega) = \frac{(\alpha(\omega) \times n(\omega))_{sol}}{n_{sol}^{exp}} - \frac{(\alpha(\omega) \times n(\omega))_{bulk}}{n_{bulk}^{exp}} \cdot \frac{\rho_{sol}^w}{\rho_{bulk}^w} \quad (\text{S.2})$$

ρ_{sol}^w and ρ_{bulk}^w are the number density of water molecules in the simulation box for the MgSO_4 solution and the bulk solvent, respectively, while n_{bulk}^{exp} and n_{sol}^{exp} are the frequency-independent refractive indices of bulk water and MgSO_4 solutions, respectively, derived as described above.

Defining a stable solvent shared ion pair

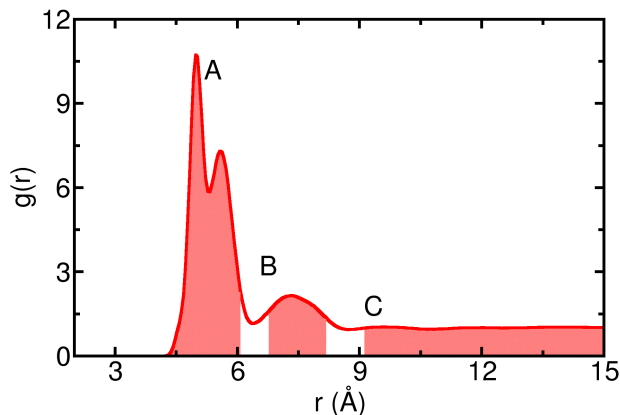


Figure S2: $\text{Mg}^{2+} \cdots \text{SO}_4^{2-}$ radial distribution function from simulations at $m = 0.5 \text{ mol}\cdot\text{kg}^{-1}$. The distance r is measured between the cation and the sulfur atom of the anion. The shaded areas correspond to stable states: (A) solvent shared ion pair; (B) solvent separated ion pair; (C) unbound.

Figure S2 shows the anion-cation radial distribution function from simulations of a MgSO_4 solution with a molality of $0.5 \text{ mol}\cdot\text{kg}^{-1}$. The shaded regions correspond to the different stable states defined using the stable states picture of Northrup and Hynes⁵. In this framework, the configurations very close to the minima of the radial distribution function are excluded from any state, because of the rapid oscillations around the minima. Instead, the boundaries of the stable states are defined based on the position of the geometric mean of consecutive maxima and minima of the radial distribution function. The calculations of the VDOS were done on species involved in stable solvent shared ion pairs. These ion pairs were defined as those belonging to region A in Figure S2 at $t=0$, and that do not cross into region B within 20 ps.

THz absorption spectra of MgCl_2 and Na_2SO_4 solutions

Magnesium chloride and sodium sulfate with a purity higher than 99 %, were purchased from Sigma Aldrich and used without further purification. We prepared the aqueous salt solutions at different concentrations and measured their mass densities in the same way as for MgSO_4 solutions.

The absorption spectra were acquired at 293 K in the frequency range $50\text{--}640 \text{ cm}^{-1}$ and the effective ionic absorption coefficients with respect to bulk water were

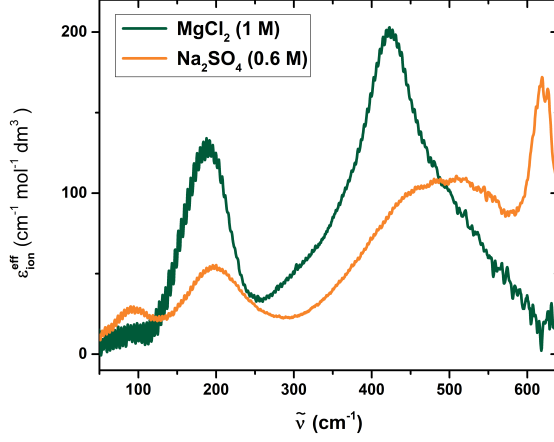


Figure S3: Effective ionic absorption spectra of MgCl_2 solution at $1 \text{ mol}\cdot\text{dm}^{-3}$ and Na_2SO_4 solution at $0.6 \text{ mol}\cdot\text{dm}^{-3}$.

obtained, as described in the Materials and Experimental Methods Section and Ref.¹. In Figure S3, the effective extinction coefficients of a MgCl_2 solution at $c_s=1 \text{ mol}\cdot\text{dm}^{-3}$ and of a Na_2SO_4 solution at $c_s=0.6 \text{ mol}\cdot\text{dm}^{-3}$ are shown ($\epsilon_{\text{ion}}^{\text{eff}} = \frac{\alpha_{\text{ion}}^{\text{eff}}}{c_s}$, see also Eqs. 2 and Ref. Schwaab *et al.*¹).

For sodium sulfate, we can assign the peak around 80 cm^{-1} to Na^{+6} ; the peak around 200 cm^{-1} is a hydrated sulfate mode and the broad band around 520 cm^{-1} likely arises from a hydration water mode of both anion and cation, by comparison with other sodium and sulfate salts¹. For MgCl_2 , the two peaks at $\approx 180 \text{ cm}^{-1}$ and $\approx 420 \text{ cm}^{-1}$ are consistent, although red-shifted, with the rattling modes of Mg^{2+} within its hydration shell (θ - and Ψ -modes), as calculated in Ref. Funkner *et al.*⁷.

Projection of the SIP trajectories

Previous experimental and simulation work by some of us indicated that in MgCl_2 solutions, magnesium coordinates 6 water molecules in the first hydration layer ($\text{Mg}^{2+}(\text{H}_2\text{O})_6$) and has two IR-active collective vibrations⁷. Those were defined as the θ -mode at 250 cm^{-1} , and the Ψ -mode at 600 cm^{-1} , respectively, and were attributed to the cation rattling within its hydration cage. The experimental modes (see Figure S3), are red-shifted relative to our prior calculations⁷ by a factor of 1.3, i.e., as $\tilde{\nu}_{\text{sim}} = 1.3 \tilde{\nu}_{\text{exp}}$.

For MgSO_4 , we projected the SIP trajectories on the modes of the $\text{Mg}^{2+}(\text{H}_2\text{O})_6$ complex, following the same procedure described in Ref. Funkner *et al.*⁷. The

results of this projection, shown in Figure 6 in the Main Text, clearly indicate that for MgSO_4 the main resonances of the θ and the Ψ modes can be found at 300 cm^{-1} and 480 cm^{-1} , respectively. In addition, both modes now display double peaks. These differences relative to our prior calculations reflect the different molecular models used in each case. It is worth noticing that the IR activity is simply due to the symmetry of the mode and there is no assignment of the IR cross section, i.e., how active they are. Assuming a redshift similar to that observed for MgCl_2 solutions, there is a qualitative agreement between these projected modes and the peaks observed in the experimental absorption spectra of MgSO_4 . This supports our proposed scenario that the formation of MgSO_4 solvent shared ion pairs has limited impact in the hydration layer of magnesium.

References

- [1] G. Schwaab, F. Sebastiani and M. Havenith, *Angew. Chem. Int. Ed.*, 2019, **58**, 3000–3013.
- [2] S. I. Mamatkulov, K. F. Rinne, R. Buchner, R. R. Netz and D. J. Bonthuis, *J. Chem. Phys.*, 2018, **148**, 222812.
- [3] P. S. Ray, *Applied Optics*, 1972, **11**, 1836.
- [4] J. E. Bertie and Z. Lan, *Appl. Spectrosc.*, 1996, **50**, 1047–1057.
- [5] S. H. Northrup and J. T. Hynes, *J. Chem. Phys.*, 1980, **73**, 2700–2714.
- [6] P. Schienbein, G. Schwaab, H. Forbert, M. Havenith and D. Marx, *J. Phys. Chem. Lett.*, 2017, **8**, 2373–2380.
- [7] S. Funkner, G. Niehues, D. A. Schmidt, M. Heyden, G. Schwaab, K. M. Callahan, D. J. Tobias and M. Havenith, *J. Am. Chem. Soc.*, 2012, **134**, 1030–1035.